1521-0103/380/3/202–209$35.00
The Journal of Pharmacology and Experimental Therapeutics

dx.doi.org/10.1124/jpet.121.000998
J Pharmacol Exp Ther 380:202–209, March 2022

The Skeletal Muscle Relaxer Cyclobenzaprine Is a Potent Non-Competitive Antagonist of Histamine H1 Receptors

Kirti Singh,[1] Ilya S. Senatorov,[1,2] Ameneh Cheshmehkani,[3] Priyanka F. Karmokar, and Nader H. Moniri

Department of Pharmaceutical Sciences, College of Pharmacy, Mercer University Health Sciences Center, Mercer University, Atlanta, Georgia (K.S., I.S.S., A.C., P.F.K., N.H.M.) and Department of Biomedical Sciences, School of Medicine, Mercer University Health Sciences Center, Mercer University, Macon, Georgia (N.H.M.)

Received October 28, 2021; accepted January 2, 2022

ABSTRACT

Cyclobenzaprine is a tricyclic dimethylpropanamine skeletal muscle relaxant, which is used clinically to decrease muscle spasm and hypercontractility, as well as acute musculoskeletal pain. Although the absolute mechanism of action of cyclobenzaprine remains elusive, it is known to mediate its effects centrally via inhibition of tonic somatic motor function, likely through modulation of noradrenergic and serotonergic systems. While cyclobenzaprine is effective as a muscle relaxant, greater than 30% of patients experience drowsiness and sedative-hypnotic effects, yet the mechanisms that cause this adverse effect are also undescribed. Based on this common adverse effect profile and the structural similarity of cyclobenzaprine to tricyclic antidepressants, as well as ethanolamine first-generation antihistamines, we hypothesized that cyclobenzaprine facilitates sedative effects via off-target antagonism of central histamine H1 receptors (H1Rs). Here, for the first time, we present data that demonstrate that cyclobenzaprine exhibits low nanomolar affinity for the cloned human H1R, as well as that expressed in both rat and mouse brain. Using saturation radioligand binding, we also demonstrate that cyclobenzaprine binds to the H1R in a noncompetitive manner. Similarly, functional assays measuring both Ca^{+2} influx and novel TRUPATH G-protein subunit bioluminescence resonance energy transfer biosensors reveal that cyclobenzaprine also blocks histamine-mediated H1R functional activity in a noncompetitive manner, whereas the classical H1R antagonist diphenhydramine does so competitively. Given that cyclobenzaprine readily crosses the blood-brain barrier and its muscle relaxant effects occur centrally, our data suggest that off-target central antagonism of H1R by cyclobenzaprine facilitates the significant sedative effect of this agent seen in patients.

SIGNIFICANCE STATEMENT

Cyclobenzaprine, a clinically used muscle relaxant that is strongly linked to sedation, demonstrates high-affinity noncompetitive antagonism at the histamine H1 receptor. This effect likely modulates the high degree of sedation that patients experience.

Introduction

Cyclobenzaprine, 3-(5H-dibenzo[a,d] cyclohepten-5-ylidene)-N, N- dimethyl-1-propanamine hydrochloride (Fig. 1), initially branded in the United States as Flexeril, is a skeletal muscle relaxer used clinically to decrease muscle spasm and muscle hypercontractility, as well as to treat acute pain due to musculoskeletal conditions (Share and McFarlane, 1975). Although the absolute mechanism of action of cyclobenzaprine remains elusive, it is known to act centrally within the brainstem to decrease efferent α and γ spinal motor neurons that regulate muscle reflex and activity (Barnes, 1976; Barnes and Adams, 1978). The locus coeruleus, which drives central noradrenergic neurotransmission, was initially postulated to be the primary site of central cyclobenzaprine action, where it was shown to facilitate decreases in noradrenergic excitation and outflow (Gintautas and Barnes, 1979; Barnes et al., 1980; Lang and Barnes, 1982; 1983). Subsequently, many decades later, it was discovered that cyclobenzaprine can also act via antagonism of serotonin 5-HT_2 receptors to block descending serotoninergic pathways, which inhibit mono- and polysynaptic reflexes within the spinal cord to decrease pain transmission (Honda et al., 2003).

Although cyclobenzaprine is generally well tolerated and has an acceptable safety profile, it also antagonizes α1-adrenergic receptors, leading to vasodilation and subsequent reflex tachycardia, and it also commonly causes xerostomia (i.e., dry mouth), mydriasis (i.e., dilation of the pupils), and gastrointestinal and urinary dysfunction, as well as tachycardia,

This work was not supported through external funding sources.
None of the authors have any conflicting interests to declare.
[1]K.S. and I.S.S. contributed equally to this work.
[2]Current Affiliation: Laboratory of Genitourinary Cancer Pathogenesis, Center for Cancer Research, National Cancer Institute, Bethesda, Maryland
[3]Current Affiliation: Department of Chemistry and Physics, University of Tennessee at Chattanooga, Chattanooga, Tennessee
Preliminary findings from a portion of this work were presented at the *Experimental Biology 2021 Meeting;* 2021 Apr 27–30; held virtually.
dx.doi.org/10.1124/jpet.121.000998.

ABBREVIATIONS: BRET, bioluminescence resonance energy transfer; BSA, bovine serum albumin; CI, confidence interval; DMEM, Dulbecco's modified Eagle's medium; E_{max}, maximal efficacy; GPCR, G-protein-coupled receptor; H1R, histamine H1 receptor; HEK, human embryonic kidney; pA2, antagonist potency.

secondary to anticholinergic effects due to antagonism of muscarinic acetylcholine receptors (Aronson, 2016). Importantly, upwards of 39% of all patients who take cyclobenzaprine exhibit significant drowsiness, sedation, and somnolence (Teva Pharmaceuticals USA, Inc., 2013), which by far represent the most commonly encountered adverse effects, and which significantly limits tolerability and the feasibility of continued clinical use.

Despite nearly 50 years of clinical utilization, the mechanisms behind the sedative and somnolence inducing effects of cyclobenzaprine are completely unstudied and have only been assumed to be due to the anticholinergic effect. Cyclobenzaprine shares structural homology with the highly sedating first-generation over-the-counter ethanolamine-based histamine H1 receptor (H1R) antagonists (i.e., antihistamines) such as diphenhydramine (e.g., Benadryl), triprolidine (e.g., Actifed), and doxylamine (e.g., Unisom and a component of Nyquil) (Fig. 1). In addition, cyclobenzaprine shares structural similarity with several clinically used tricyclic antidepressants, (Fig. 1) including imipramine, amitriptyline, nortriptyline, and doxepin, that are also all highly sedating, and which, also exhibit H1R antagonism. Based on this high degree of structural homology to known sedating histamine H1 receptor antagonists, we hypothesized that the sedative and somnolence effects of cyclobenzaprine are mediated by off-target antagonism of central H1R. Here, using a variety of receptor-binding and functional assays, we report for the first time that cyclobenzaprine is a potent noncompetitive antagonist of H1R, and that indeed, the sedative effects seen clinically are likely modulated by the blockade of central H1R.

Materials and Methods

Reagents and Chemicals. DNA encoding the wild-type human histamine H1 receptor in the pcDNA3.1+ plasmid was purchased from the Missouri S&T cDNA Resource Center (https://www.cdna.org). Cyclobenzaprine hydrochloride (PubChem CID: 22576), diphenhydramine hydrochloride (PubChem CID: 8980), and other chemicals were obtained at the highest available purity from Sigma-Aldrich (St. Louis, MO). Histamine dihydrochloride (PubChem CID: 5818) was obtained from Acros Organics (Fair Lawn, NJ). The TRUPATH biosensors were a kind gift from the laboratory of Dr. Bryan Roth (UNC-Chapel Hill, Chapel Hill, NC; Addgene kit #1000000163) (Olsen et al., 2020). [^{3}H]-Mepyramine (PubChem CID: 4992; NET594250UC) was purchased from Perkin Elmer (Waltham, MA).

Animals. Rat cortex was obtained fresh from young adult (125–150 g) male Sprague Dawley rats that were obtained from Charles River Laboratories (Wilmington, MA) and housed for at least 1 week before use under controlled environmental conditions (20–22°C, 40%–50% humidity, lights on from 0700 to 1900 hours). The animal use protocol was approved by the Mercer University Institutional Animal Care and Use Committee. Animals had free access to commercial food pellet and fresh tap water. Mouse cortex was dissected from flash-frozen brains from male mice obtained commercially from Innovative Research (Novi, MI).

Cell Culture, Transfection, and Treatment. Human embryonic kidney (HEK293) cells were obtained from ATCC (American Type Culture Collection, Manassas, VA) and were cultured in 100-mm plates containing Dulbecco's modified Eagle's medium (DMEM) and supplemented with 10% fetal bovine serum and 1% penicillin-streptomycin (Life Technologies, Grand Island, NY). The AequoScreen HEK293/Gα_{16} parental cell line (ES-000-A26) was purchased from Perkin Elmer. Transient transfections were performed using LipoD293 reagent (Signagen Laboratories, Gaithersburg, MD) according to the manufacturer's directions, exactly as we have previously reported (Burns and Moniri, 2011; Singh and Moniri, 2012; Burns et al., 2014; Senatorov et al., 2020).

Radioligand Competition and Saturation Binding Assays. Competition binding assays were performed as we have described previously in detail (Booth et al., 2002; Moniri et al., 2004; Moniri and Daaka, 2007). Briefly, HEK293 cells were transfected with 5 μg of H1R in 10-cm dishes using LipoD293 reagent according to the manufacturer's instructions. Cells were harvested 48 hours after transfection by detaching from the plate with ice-cold phosphate-buffered saline (pH 7.5) and were centrifuged at 1000 rpm for 10 minutes. The resulting pellet was suspended again in ice-cold buffer, homogenized with 10 strokes of a Wheaton Teflon-glass homogenizer, and centrifuged at 35,000 × g for 20 minutes at 4°C. The resulting pellet was resuspended in buffer at 1 ml per dish and used fresh or stored at −80°C for future use. Membrane aliquots (25 μg) were incubated with K_D concentration of [^{3}H]-mepyramine (~1 nM) and varying concentrations of test agent (0.001–100 μM) for 1 hour at 25°C. Reactions were terminated by rapid filtration over Whatman GF/C filters followed by washing in ice-cold buffer supplemented with 0.1% bovine serum albumin (BSA). Filters were counted for radioactivity using liquid scintillation spectrometry (Packard 2250 Liquid Scintillation Counter, Waltham, MA), and results are expressed as the percentage of specific binding, which is defined by subtracting nonspecific binding in the presence of 100 μM diphenhydramine. Protein content was analyzed using DC Protein Assay (Bio-Rad, Hercules, CA). Resulting inhibition data were analyzed by nonlinear regression using the sigmoidal curve-fitting algorithms in GraphPad Prism 9 (GraphPad Software, San Diego, CA) to determine half-maximal inhibitory concentration (IC_{50}) and Hill slopes (n_H). Affinity is expressed as a measure of the exact concentration of radioligand per experiment using the following equation:

$$K_i = IC_{50}/(1 + L/K_D),$$

where L is the concentration of radioligand in each replicate, having affinity K_D (Cheng and Prusoff, 1973). Each experimental condition was run in triplicate, and each experiment was performed a minimum of three times to determine S.D. Saturation binding experiments were conducted as we have reported previously (Moniri et al., 2004). Briefly, cells were transfected with 2 μg of H1R and prepared as described above, except membranes were prepared in buffer containing 25 mM Tris-HCl, 4mM $MgCl_2$ (pH 7.5) and the filters were washed with identical buffer containing 0.1% BSA. Filters were dried on a hot plate for 20 minutes at 80–90°C, and radioactivity was assessed using a MicroBeta2 2450 Microplate counter (Perkin Elmer, Waltham, MA). Specific binding was obtained by subtracting nonspecific binding in the presence of diphenhydramine from total binding, as above.

TRUPATH Bioluminescence-Resonance Energy Transfer. Bioluminescence-resonance energy transfer (BRET) experiments were performed based on those described by others (Olsen et al., 2020) and similar to our previous studies (Singh and Moniri, 2012; Senatorov et al., 2020). Briefly, cells were washed three times, dislodged with BRET buffer (140 mm NaCl, 2.7 mM KCl, 1 mM $MgCl_2$, 1 mM $CaCl_2$, 0.37 mM NaH_2PO_4, 24 mM $NaHCO_3$, 25 mM HEPES, 0.1% Glucose, pH 7.4), centrifuged at 0.5 × g for 5 minutes, and resuspended at 1 × 10^6 cells/ml. Fifty thousand cells were loaded per well of a white 96-well plate and incubated with various concentrations of test agents for 10 minutes, followed by 5-minute equilibration with Coelenterazine 400A (DeepBlueC) (5 μM) (Biotium, Hayward, CA). Cells were then stimulated with histamine for 5 minutes before detection of emission at 410 nm (RLuc8-DeepBlueC) and 515 nm (GFP2) using a Mithras LB940 plate reader (Berthold Technologies, Oak Ridge, TN). BRET2 signal was calculated as a ratio of GFP2 emission over RLuc8 emission, and results are expressed normalized to the maximal histamine response elicited. IC_{50} was determined using GraphPad Prism 9, and data are expressed as mean ± S.D. for representative experiments repeated at least three independent times. Antagonist potency, reported as pA2, was measured using the Gaddum/Schild EC_{50} Shift method and calculated in GraphPad Prism 9, using the output EC_{50}

for histamine alone, B = antagonist concentration used, and a Schild slope of 1.0. Values for bottom, top, and KB were best-fit by Prism, and $LogEC_{50}$, bottom, top, and Hill slope were shared constraints.

Intracellular Ca^{+2} Luminescence. HEK293+$G\alpha_{16}$ AequoScreen parental cell lines (Perkin Elmer, Waltham, MA) were cultured in 100-mm tissue culture plates under Bleocin selection (MilliporeSigma, Burlington, MA) in DMEM and supplemented with 10% FBS and 1% penicillin-streptomycin in a humidified atmosphere with 5% CO_2 at 37°C. Cells were transfected with 5 μg H1R as above, and experiments were performed 48 hours post-transfection. Cells were resuspended (3×10^5 cells/ml) in assay buffer (phenol-free DMEM, 25mM HEPES, 5 μM coelenterazine-h, 0.1% BSA) and placed in the dark with constant agitation for 4 hours. Cells were then diluted 3-fold in assay buffer without coelenterazine and incubated for an additional 60 minutes, followed by pretreatment with vehicle or test agent for 10 minutes. Cells were then placed into white 96-well plates preloaded with serial dilutions of histamine, and total luminescence was read for 30 seconds using a Tecan M200 Infinite Pro plate reader (Tecan, Mannedorf, Switzerland). EC_{50} was determined using GraphPad Prism 9, and data are expressed as mean ± S.D. for representative experiments repeated at least three independent times. Antagonist potency, reported as pA2, was measured using the Gaddum/Schild EC_{50} Shift method and calculated in GraphPad Prism 9, using the output EC_{50} for histamine alone, B = antagonist concentration used, and a Schild slope of 1.0. Values for bottom, top, and KB were best-fit by Prism, and $LogEC_{50}$, bottom, top, and Hill slope were shared constraints.

Data Analysis. Results were imported and graphed using GraphPad Prism 9. Data are expressed as mean ± S.D. or normalized as shown in the figures. Where shown, pEC_{50} ± S.D. was calculated using the sigmoidal concentration-response algorithm in Prism, using pooled data from all experiments (n denoted in figure legends). For IC_{50} and pA2 calculations, the means from each individual experiment performed in triplicate were pooled (n = 3–5 as shown in the legends). Where not visible, error bars fall within the symbol size. Ninety-five percent confidence intervals from Prism outputs are described as CI in the results. Statistical analysis for binding affinity in Table 1 was performed using two-tailed, paired Student's t test. Statistical analysis for figures was performed in GraphPad Prism 9 using one-way analysis of variance and post-hoc Tukey analysis. Statistical significance is represented as a descriptive (nonhypothesis testing) P-value using a single symbol for $P < 0.05$, a double symbol for $P < 0.01$, and a triple symbol for $P < 0.001$, as noted in the figure legends.

Results

Cyclobenzaprine Is a High-Affinity Histamine H1 Receptor Ligand. To determine if cyclobenzaprine binds to histamine H1 receptors, we performed competition binding experiments assessing the ability of cyclobenzaprine to displace the standard H1R radioligand [^{3}H]-mepyramine and compared this effect to the classical high-affinity H1R antagonist diphenhydramine. To avoid the confounding variables of other receptor systems, transporters, and circuits of the brain, we first assessed binding of cyclobenzaprine in a clonal HEK293 cell line that does not endogenously express H1R, in which we transiently express the receptor (HEK293-H1R). In these cells, cyclobenzaprine fully displaces [^{3}H]-mepyramine from the H1R with a K_i of 3.2 ± 1.0 nM and a Hill slope of −1.1 ± 0.2 (Fig. 1A; Table 1). The displacement effects of cyclobenzaprine were apparent even at concentrations as low as 10 pM (–11 point, Fig. 1) in HEK293 cells. The Hill slope was similar to that of diphenhydramine and characteristic of antagonist binding to a uniform population of sites of a GPCR (Hall and Langmead, 2010). Although diphenhydramine also fully displaced [^{3}H]-mepyramine from the H1R, it did so with 2.3-fold less affinity (K_i 7.4 ± 0.8) (Fig. 1A; Table 1). This difference in affinity was also evident at both the mouse and rat cortical H1R, where cyclobenzaprine was 5-fold (9.2 ± 2.5 nM vs. 45.6 ± 8.6 nM) and 7-fold (7.1 ± 0.5 nM vs. 52.7 ± 13.4 nM) more potent than diphenhydramine, respectively (Fig. 1A; Table 1). Hill slopes for cyclobenzaprine were similar to diphenhydramine in both mouse (−0.93 ± 0.04 and −0.90 ± 0.03, respectively) and rat (−1.1 ± 0.02 and −0.96 ± 0.1, respectively) H1R (Table 1).

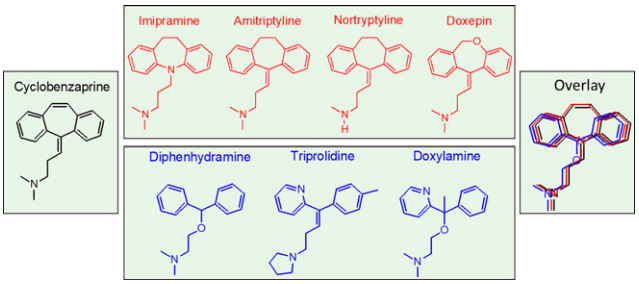

Fig. 1. Structures of cyclobenzaprine (left) compared with the known sedating histamine H1 antagonists belonging to the tricyclic antidepressant family (top) or the first-generation arylethanolamine histamine H1 receptor antagonists (bottom). An overlay of cyclobenzaprine with a member of each is at right.

Cyclobenzaprine Is a Non-competitive Antagonist of Histamine H1 Receptors. Previously, it was established that ethanolamine-based H1R antagonists such as diphenhydramine and triprolidine act competitively at the same site on the H1R that is labeled by [^{3}H]-mepyramine (Chang et al., 1978; 1979; Tran et al., 1978), and our own previous data mirror these (Moniri et al., 2004). To determine the nature of the binding interaction between cyclobenzaprine and the site labeled by [^{3}H]-mepyramine, we performed saturation binding experiments with increasing concentrations of [^{3}H]-mepyramine in the absence or presence of cyclobenzaprine at approximately one-third and 3-fold its K_i concentration (i.e., 1 and 10 nM). Results of these experiments show that [^{3}H]-mepyramine exhibits a K_D of 8.2 ± 1.3 nM in our transient expression system, similar to what we and others have reported elsewhere for the human receptor expressed in clonal

TABLE 1
Binding affinities (K_i) and Hill slopes (n_H) of cyclobenzaprine and diphenhydramine at the human cloned H1R expressed in HEK293 cells and the mouse and rat cortical H1R

	HEK293-H1R		Mouse Cortex		Rat Cortex	
	K_i (nM)	n_H	K_i (nM)	n_H	K_i (nM)	n_H
Cyclobenzaprine	3.2 ± 1.0	−1.1 ± 0.2	9.2 ± 2.5	−0.93 ± 0.04	7.1 ± 0.5	−1.1 ± 0.02
Diphenhydramine	7.4 ± 0.8*	−0.99 ± 0.2	45.6 ± 8.6*	−0.90 ± 0.03	52.7 ± 13.4*	−0.96 ± 0.1

*$P < 0.05$ vs. cyclobenzaprine

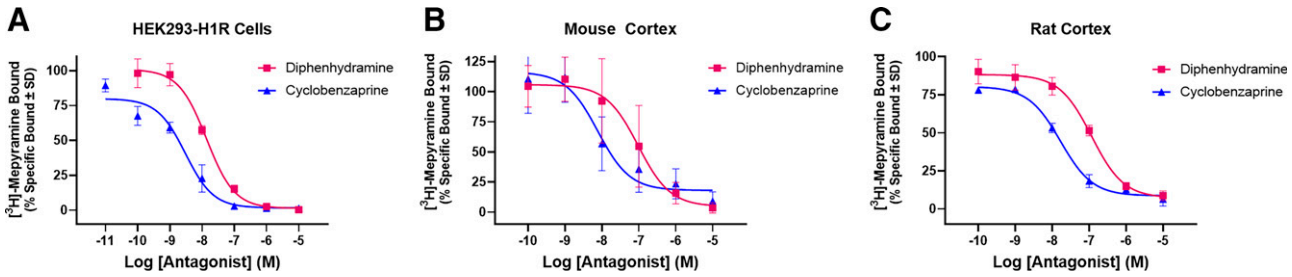

Fig. 2. Competition binding assays of cyclobenzaprine (blue) or the classical competitive H1R antagonist diphenhydramine (red) at H1R transiently expressed in HEK293 cells (A), mouse cortex (B), or rat cortex (C). Aliquots of each membrane preparation (25 μg) were incubated with K_D concentration of [^{3}H]-mepyramine (~1 nM) and varying concentrations of test agent (0.001–100 μM) for 1 hour at 25°C and filtered and quantified as described in the materials and methods. Diphenhydramine (100 μM) was used to define nonspecific binding, which was subtracted from the total binding of [^{3}H]-mepyramine to calculate specific binding. The affinity of cyclobenzaprine, defined as K_i, was 3.2 ± 1.0, 9.2 ± 2.5, and 7.1 ± 0.5 nM (A–C) for the human, mouse, and rat receptor, respectively, whereas the affinity of diphenhydramine was 7.4 ± 0.08, 45.6 ± 8.6, and 52.7 ± 13.4 nM, respectively. Each experiment was performed in triplicate (n = 4–5).

cell lines (Moguilevsky et al., 1994; 1995; Booth et al., 2002; Moniri and Booth, 2004; Moniri et al., 2004; Booth and Moniri, 2005). The presence of 1 or 10 nM cyclobenzaprine significantly reduced [^{3}H]-mepyramine binding to the H1R, with specific [^{3}H]-mepyramine binding detected only at concentrations above 10 nM in the presence of cyclobenzaprine (P = 0.01 ANOVA) (Fig. 3A). Importantly, cyclobenzaprine dose-dependently decreased the B_{max} of [^{3}H]-mepyramine; however, this was most evident at the highest concentration of radioligand (~14 nM), where [^{3}H]-mepyramine binding was reduced by 41% in the presence of 1 nM and by 73% in the presence of 10 nM cyclobenzaprine (P = 0.003 ANOVA) (Fig. 3B). [^{3}H]-mepyramine binding at concentrations below 14 nM was essentially fully blocked by the presence of cyclobenzaprine. Importantly, the observed reduction of B_{max} is consistent with binding of cyclobenzaprine to a distinct site of the H1R from which [^{3}H]-mepyramine binds in a non-competitive manner, similar to that which has been described for other nonclassical H1R ligands (Moniri et al., 2004).

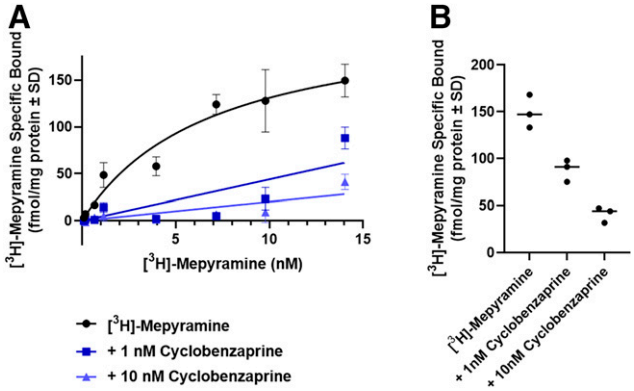

Fig. 3. Saturation binding of [^{3}H]-mepyramine was inhibited in the presence of 1 nM or 10 nM cyclobenzaprine in a non-competitive manner. Aliquots of each membrane preparation were incubated with shown concentrations of [^{3}H]-mepyramine in the absence or presence of either concentration of cyclobenzaprine for 1 hour at 25°C and filtered and quantified as described in the materials and methods. (A) [^{3}H]-mepyramine exhibited a K_D of 8.2 ± 1.3 nM and the presence of 1 or 10 nM cyclobenzaprine significantly reduced [^{3}H]-mepyramine binding to the H1R, with specific [^{3}H]-mepyramine binding detected only at concentrations above 10 nM in the presence of cyclobenzaprine (P = 0.01 ANOVA). (B) The B_{max} of [^{3}H]-mepyramine was reduced by 41% in the presence of 1 nM and by 73% in the presence of 10 nM cyclobenzaprine (P = 0.003 ANOVA). Each experiment was performed in triplicate (n = 3–5).

Cyclobenzaprine Inhibits H1R Function in a Non-competitive Manner. Since H1R primarily couples to the $G\alpha_{q/11}$-PLC/IP_3-DAG signaling cascade that facilitates intracellular Ca^{+2} release, we examined the functional effects of cyclobenzaprine compared with diphenhydramine upon agonism of the H1R with the endogenous agonist histamine, using the luminescent Ca^{+2} AequoScreen assay. Agonism of untransfected parental HEK293 (+$G\alpha_{16}$) AequoScreen cells with histamine elicited no luminescence (data not shown). On the contrary, in cells transfected with H1R, histamine elicited a sigmoidal dose-response of Ca^{+2} luminescence with an pEC_{50} of −6.1 ± 0.1 (i.e., 764 nM) (Fig. 4, A and B). In the presence of the classical competitive H1R antagonist diphenhydramine, the histamine curve was expectedly right-shifted and the agonist pEC_{50} decreased to −5.0 (CI: −5.5 to −4.4) and −3.7 (CI: −3.2 to −4.3) in the presence of 1 nM and 10 nM diphenhydramine, respectively (P < 0.01 ANOVA) (Fig. 4A). Notably, the maximal histamine efficacy (E_{max}) was not altered by either concentration of diphenhydramine, consistent with competitive diphenhydramine interaction at the H1R at a site that overlaps the histamine binding site.

The Ca^{+2}-inducing effects of histamine were similarly right-shifted in the presence of 100 pM, 1 nM, or 10 nM cyclobenzaprine, with pEC_{50} shifts from −6.1 to −4.1, −2.3, and −0.14, respectively, although the last point lacked confidence due to abolishment of the curve (P < 0.001 ANOVA; CI: −6.3 to −5.8, −4.3 to −3.9, and −3.5 to −2.2, respectively) (Fig. 4B). When potency values were reported as pA2, which is defined as the negative logarithm of the concentration of antagonist needed to shift the curve by a factor of 2, cyclobenzaprine yielded a calculated pA2 of 11.92 (1.2 pM), whereas diphenhydramine yielded a calculated pA2 of 10.15 (70 pM), demonstrating that cyclobenzaprine is approximately 70-fold more potent at inhibiting histamine-induced Ca^{+2} release at H1R compared with diphenhydramine. Importantly, and contrary to that seen with diphenhydramine, cyclobenzaprine treatment also significantly decreased the E_{max} of the histamine-induced effect to 60%, 30%, and 15% of the maximal histamine response in the presence of 100 pM, 1 nM, and 10 nM of the antagonist, respectively (P < 0.001 ANOVA; CI: 43.2 – 74.4, 25.7 – 33.4, and 9.6 – 20.5, respectively) (Fig. 4B). Together, these data suggest that cyclobenzaprine decreases H1R function via non-competitive interactions at a distinct site from where histamine and mepyramine bind.

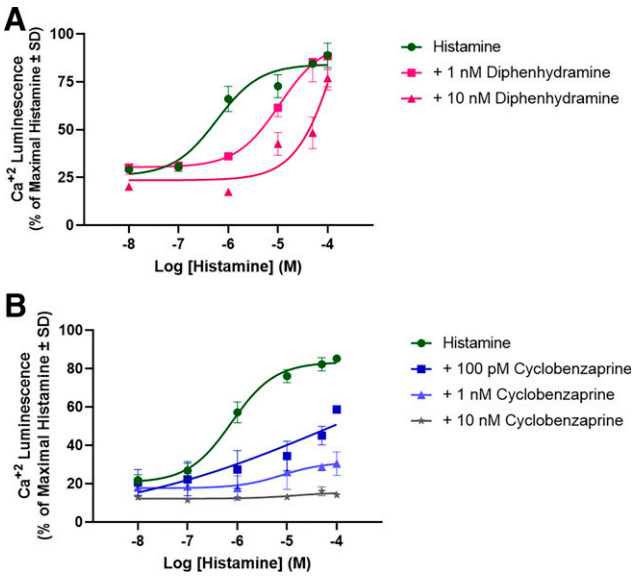

Fig. 4. Histamine-induced Ca^{+2} luminescence is inhibited by cyclobenzaprine in a non-competitive manner. (A and B) Histamine induces H1R-dependent Ca^{+2} luminescence in HEK293 (+$G\alpha_{16}$) AequoScreen cells with a pEC_{50} of −6.1 ± 0.1 (i.e., 764 nM) (green). No histamine-induced effect was seen in cells that were not transfected with H1R (not shown). (A) The competitive H1R antagonist diphenhydramine right-shifted the histamine effect, and the agonist pEC_{50} decreased to −5.0 (CI: −5.5 to −4.4) and −3.7 (CI: −3.2 to −4.3) in the presence of 1 nM and 10 nM diphenhydramine, respectively ($P < 0.01$ ANOVA). The E_{max} of the histamine effect was not altered by either concentration of diphenhydramine, consistent with the known competitive interaction of diphenhydramine with the H1R. The calculated pA2 of diphenhydramine for this effect was 10.15 (70 pM). Each experiment was performed in triplicate ($n = 4$). (B) In the presence of 100 pM, 1 nM, or 10 nM cyclobenzaprine, the histamine pEC_{50} shifts from −6.1 to −4.1, −2.3, and −0.14, respectively, although the last point lacked confidence due to abolishment of the curve ($P < 0.001$ ANOVA; CI: −6.3 to −5.8, −4.3 to −3.9, and −3.5 to −2.2, respectively). The calculated pA2 of cyclobenzaprine for this effect was 11.92 (1.2 pM). The E_{max} of the histamine-induced effect decreased to 60%, 30%, and 15% of the maximal histamine response in the presence of 100 pM, 1 nM, and 10 nM of cyclobenzaprine, respectively ($P < 0.001$ ANOVA; CI: 43.2 – 74.4, 25.7 – 33.4, and 9.6 – 20.5, respectively). Each experiment was performed in triplicate ($n = 5$).

Cyclobenzaprine Inhibits H1R G-Protein Signaling in a Non-competitive Manner. To confirm these results, we next assessed the effects of diphenhydramine compared with cyclobenzaprine in the novel TRUPATH assay that examines agonist-induced G-protein subunit signaling. The H1R is well described to couple to heterotrimeric $G\alpha_{q/11}$ proteins that are also comprised of $G\beta_1$ or $G\beta_2$ and $G\gamma_1$ or $G\gamma_2$ subunits. Others have shown that the $G\beta_1/G\gamma_1$ combination does not significantly impact agonist-independent H1R activity while it preserves native agonist-induced signals (Bakker et al., 2001; Adjobo-Hermans et al., 2011). Hence, we performed BRET experiments with TRUPATH plasmids encoding Gαq fused to RLuc8 (Gαq-RLuc8), $G\gamma_1$ fused to GFP2 ($G\gamma_1$-GFP2), and $G\beta_1$ (Olsen et al., 2020). In this experiment, unagonized H1R retains the Gαq-RLuc8/$G\gamma_1$-GFP2/$G\beta_1$ in the heterotrimeric state that elicits BRET transmission from the GFP donor to the RLuc acceptor, emitting a net BRET signal. Upon agonism with histamine, the displacement of the heterotrimer into distinct Gαq-RLuc8 and $G\gamma_1$-GFP2/$G\beta_1$ subunits leads to loss of the fluorescence-induced BRET signal, allowing us to measure agonist, and in turn, antagonist function at G-protein activation. Results of this experiment demonstrate that as expected, histamine elicits a dose-dependent decrease in net BRET with a pIC_{50} of −5.3 ± 0.13 (CI: −5.5 to −5.1) (Fig. 5, A and B). In the presence of 10 nM, 1 nM, or 1 μM diphenhydramine, the histamine-induced decrease in Gαq-RLuc8/$G\gamma_1$-GFP2 BRET was right-shifted but surmountable as the histamine concentration increased, as expected for a competitive antagonist (Fig. 5A). pIC_{50}s were shifted to −5.6 ± 0.5, −5.1 ± 0.3, and −3.9 ± 0.2 in the presence of these concentrations of diphenhydramine, respectively, with a corresponding pA2 value of 7.6 (25 nM) and a slope (−1.16 ± 0.07) that again, corresponds to the effects of a competitive antagonist.

On the contrary, in the presence of 10 nM, 100 nM, or 1 μM cyclobenzaprine, the histamine-induced decrease in Gαq-RLuc8/$G\gamma_1$-GFP2 BRET was both right-shifted and insurmountable, confirming a non-competitive effect (Fig. 5B). pIC_{50}s were shifted from −5.3 ± 0.1 to −4.9 ± 0.6 and −3.7 ± 0.2 in the presence of 10 nM and 100 nM, cyclobenzaprine, respectively, whereas the shift was incalculable for the 1 μM concentration due to flattening of the regression curve, as above. The resultant pA2 value of 8.57 (2.7 nM) corresponded

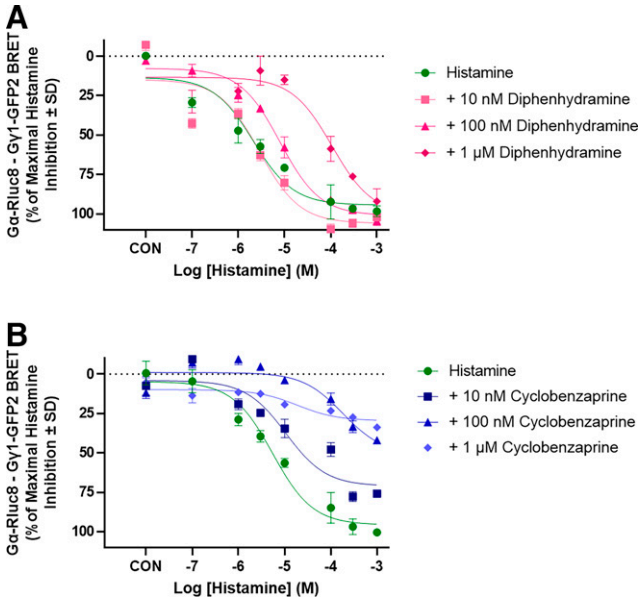

Fig. 5. Histamine-induced Gα-RLuc8 – $G\gamma_1$-GFP2 BRET is inhibited by cyclobenzaprine in a non-competitive manner. (A and B) Histamine elicits a dose-dependent decrease in net BRET with a pIC_{50} of −5.3 ± 0.13 (CI: −5.5 to −5.1). (A) In the presence of 10 nM, 1 nM, or 1 μM diphenhydramine, the histamine pIC_{50}s were shifted to −5.5 ± 0.5, −5.1 ± 0.3, and −3.9 ± 0.2, respectively, and the effects of diphenhydramine were surmountable by increasing histamine concentrations, indicative of competitive antagonism. The calculated pA2 value was 7.6 (25 nM), and the slope was −1.16 ± 0.07. Each experiment was performed in triplicate ($n = 3$), and a representative curve is shown. (B) In the presence of 10 nM, 100 nM, or 1 μM cyclobenzaprine, the histamine-induced decrease in Gαq-RLuc8/$G\gamma_1$-GFP2 BRET was both right-shifted and insurmountable, confirming a non-competitive effect. Histamine pIC_{50}s were shifted from −5.3 ± 0.1 to −4.9 ± 0.6 and −3.7 ± 0.2 in the presence of 10 nM and 100 nM cyclobenzaprine, respectively, whereas the pIC_{50} was incalculable for the 1 μM concentration due to flattening of the regression curve. The resultant pA2 value of 8.57 (2.7 nM) corresponded precisely with the affinity of cyclobenzaprine for the human H1R. The E_{max} of histamine in the presence of 10 nM, 100 nM, and 1 μM cyclobenzaprine was only 76% ± 3%, 39% ± 5%, and 33% ± 0% of that seen in the absence of antagonist, respectively. Each experiment was performed in triplicate ($n = 3$), and a representative curve from pooled experiments is shown. To ensure that the effects of the inhibition were not due to cell death induced by the vehicle, the experiment was also performed with only the highest concentration of vehicle, and these results did not affect the BRET signal (not shown).

precisely with the affinity of cyclobenzaprine for the human H1R (Fig. 2A). Importantly, and in contrast to diphenhydramine, the E_{max} of histamine in the presence of 10 nM, 100 nM, and 1 μM cyclobenzaprine was only 76% ± 3%, 39% ± 5%, and 33% ± 0% of that seen in the absence of antagonist, respectively (Fig. 5B). Since the effect in this assay is an inhibitory one, to ensure that the outcome was not due to cell death or the effects of the vehicle, we also performed the experiment in the presence of the highest concentration of vehicle alone, and these results showed no significant reduction the BRET signal (data not shown).

Discussion

Here, for the first time, we demonstrate that the skeletal muscle relaxer cyclobenzaprine, which is heavily used clinically in the settings of musculoskeletal injury and pain, is a potent non-competitive antagonist of the histamine H1 receptor. As such, our results demonstrate that the primary adverse effect encountered by patients, namely drowsiness and somnolence, is likely mediated by functional antagonism of central H1R. Although this effect would be similar to other first-generation antihistamines such as diphenhydramine, our results also demonstrate that cyclobenzaprine is 2- to 7-fold more potent than diphenhydramine, suggesting an even more significant antihistaminergic response. Interestingly, previous results of others have shown that the tricyclic-based antihistamines olopatadine and desloratidine, but not epinastine or loratidine, which also have tricyclic nuclei, inhibit histamine induced functional effects in a non-competitive manner (Matsumoto et al., 2008). The effects of olopatadine were dependent on geometric isomerism, as the E-isomer displayed competitive effects at all but the highest concentration, suggesting that the orientation of the dimethylaminopropylidene group about the double bond modulates the non-competitive effects of the former. Amitriptyline, another tricyclic agent with an sp2 hybridized dimethylaminopropylidene, but which is planar and lacks geometric isomers similar to cyclobenzaprine, was noted to exert competitive antagonism at H1R (Kachur et al., 1988), demonstrating that simple geometry about the double bond does not drive non-competitive binding interactions. Indeed, the only difference between amitriptyline and cyclobenzaprine is the additional double bond in the cycloheptene ring (Fig. 1), implying that the more rigid central ring of cyclobenzaprine can constrain conformations that exhibit unique (i.e., non-competitive) binding configurations.

Doxepin (Fig. 1), a tricyclic antidepressant and structurally similar N,N-dimethylpropylamine compound that differs from cyclobenzaprine by replacement of the cycloheptyl double bond with an ether, is one of the most potent known H1R antagonists (Kanba and Richelson, 1984; Richelson and Nelson, 1984) and is used clinically as a hypnotic for this reason, albeit at much lower doses compared with its antidepressant use. Importantly, this agent has been shown to bind to H1R in a competitive manner, at least for H1R expressed in rodent brain (Aceves et al., 1985). The crystal structure of the H1R with doxepin bound has been solved and shows that like other bioaminergic agents, doxepin's dimethylamine forms an ionic salt bridge with Asp107, which is highly conserved among bioaminergic GPCRs (Shimamura et al., 2011). Meanwhile, the tricyclic ring system sits far further (~5Å) within the H1R binding pocket compared with other GPCRs, including the β2-adrenergic receptor, dopamine D3 receptor, and α2A adrenergic receptor (Shimamura et al., 2011). Although the Z-isomer of doxepin can form a H-bond with Thr112$^{3.37}$ in TMH3 (Shimamura et al., 2011), the lack of this group in cyclobenzaprine suggests that this interaction does not exist. The presence of the additional double bond, and hence additional pi electrons, at the equivalent site in cyclobenzaprine suggests unique hydrophobic interactions, perhaps with nearby Tyr108$^{3.33}$ or Trp158$^{4.56}$, which are similarly distanced to the corresponding oxygen in doxepin, or with Phen432$^{6.52}$ or Phe435$^{6.55}$, which protrude into the doxepin binding site from the opposing side and are involved with hydrophobic interactions with the phenyl rings (Shimamura et al., 2011). Zwitterionic *N*-alkylcarboxylic acids based on the cyclobenzaprine and doxepin backbones also demonstrate potent H1R antagonistic effects, as measured by inhibition of histamine-induced contraction of guinea pig ileum, whereas increasing the length of the *N*-substituted alkyl chain upheld H1R antagonism but significantly decreased muscarinic receptor and α-adrenoreceptor antagonism (Muramatsu et al., 1993).

Our results demonstrate that cyclobenzaprine has markedly higher affinity for the H1R compared with diphenhydramine. For the human H1R, cyclobenzaprine demonstrates ~2.3-fold greater affinity than diphenhydramine, an effect that translated to a surprising 70-fold difference in the pA2 value for functional inhibition of histamine-induced Ca^{+2} signaling between the two. Interestingly, the difference in pA2 for Gα-RLuc/Gγ_1-GFP dissociation was only ~9-fold between cyclobenzaprine and diphenhydramine. This stark difference in pA2 values in the Ca^{+2} and BRET results is likely due to the nature of the aequorin-expressing HEK293 cells used in the former experiments. These cells stably express the mitochondrial aequorin Ca^{+2}-binding protein, which is highly sensitive to even small kinetic increases in Ca^{+2}, an effect that may be amplified compared with the BRET technique. The stable expression of proprietary levels of aequorin by the manufacturer, which is likely much higher compared with relatively lower (1μg per 100-mm dish) and transient levels of Gα, Gβ, and Gγ subunits transfected in the BRET assay, may also contribute to this difference. Additionally, the aequorin HEK293 cells used in the Ca^{+2} assays stably express the promiscuous Gα_{16}, which is highly efficient in coupling to phospholipase C, but importantly, previous work has shown that the potency and efficacy of GPCR agonists are significantly increased in the presence of Gα_{16}, which is used in these assays to allow for robust detection of Ca^{+2} (Stables et al., 1997; Langer et al., 2001; Zhu et al., 2008; Kurko et al., 2009). Finally, the difference in pA2 values in these experiments may also be reflective of the amplification of the signal in the presence of histamine, despite antagonist presence, as well as involvement of other G-protein subunits such as Gα_{11}, Gβ_2, Gβ_5, and Gγ_2, which are known to be implicated in histamine-induced Ca^{+2} effect (Bakker et al., 2001) but are not assessed in our Gαq/Gγ_1/β_1-based BRET assay here. Importantly, the efficacy of blockade of the histamine-induced Ca^{+2} effect mirrored that of the BRET data in that the diphenhydramine-elicited response was surmountable by increasing histamine concentrations, whereas the cyclobenzaprine-elicited response was not, in a manner consistent with non-competitive reduction in the efficacy (i.e., E_{max}) of histamine by cyclobenzaprine. Accordingly, the effects of cyclobenzaprine on both antagonism of the histamine-induced Ca^{+2} and G-protein effects appear to be mainly a

result of the decrease in E_{max}, which significantly affects the EC_{50} seen in both assays.

Given the high affinity of cyclobenzaprine for H1R, it is somewhat surprising that only 30%–40% of patients on cyclobenzaprine experience significant drowsiness and sedative-hypnotic effects. This less-than-expected proportion agrees with effects seen with other first-generation antihistamines, including diphenhydramine, and may be a result of metabolites, which in that case can cause paradoxical stimulation (de Leon and Nikoloff, 2008). In the case of cyclobenzaprine, it is known that dosage, administration, and formulation can also play a role, given the relatively slow biotransformation and accumulation of the agent. Indeed, patients on once-daily extended-release formulation exhibit effective muscle relaxation and pain management but also demonstrate very little in the way of somnolence (McCarberg et al., 2011; Teva Pharmaceuticals USA Inc., 2013) compared with those on standard three-times-daily regimens. Finally, since cyclobenzaprine acts in part via inhibition of NET and also exhibits α2-adrenoreceptor antagonism (Muramatsu et al., 1993), sedative effects may be offset by norepinephrine-mediated stimulation.

The current study explains the molecular mechanisms of the potential sedative effects of cyclobenzaprine but also demonstrates the need to use cyclobenzaprine with caution in patients on other antihistamines, particularly over-the-counter antihistamines and combination cough and cold products. In this regard, there are an abundance of case reports of cyclobenzaprine toxicities and overdoses when the agent is combined with other centrally acting depressants, including GABAergics such as benzodiazepines and alcohol (Winek et al., 1999; Spiller and Cutino, 2003; Bebarta et al., 2011). Given that histamine plays a role in the maintenance of systemic, arterial, and pulmonary blood pressure, as well as in regulating seizure susceptibility, there are also concerns about the additive effects of cyclobenzaprine and other antihistamines on blood pressure and convulsions (Bebarta et al., 2011). A recent case report documenting the fatal interaction between cyclobenzaprine and the over-the-counter H1R antagonist chlorpheniramine is illustrative of the cautions of combining these agents (Shihata, 2021).

In conclusion, our results show that the skeletal muscle relaxer cyclobenzaprine exhibits low nanomolar potency for the histamine H1 receptor, which is 2- to 7-fold higher than diphenhydramine, depending on the species. Cyclobenzaprine binds to the H1R binding pocket at a site that leads to non-competitive displacement of histamine and mepyramine, and this effect allows for non-competitive inhibition of histamine-induced functional effects via H1R, in contrast to competitive interactions seen with classical ethanolamine backbones such as diphenhydramine. As a consequence of these effects, the sedative-inducing properties of cyclobenzaprine are likely modulated by antagonism of central H1R.

Authorship Contributions

Participated in research design: Senatorov, Moniri.

Conducted experiments: Singh, Senatorov, Cheshmehkani, Karmokar.

Performed data analysis: Senatorov, Cheshmehkani, Moniri.

Wrote or contributed to the writing of the manuscript: Singh, Senatorov, Cheshmehkani, Karmokar, Moniri.

References

Aceves J, Mariscal S, Morrison KE, and Young JM (1985) The binding of doxepin to histamine H1-receptors in guinea-pig and rat brain. *Br J Pharmacol* **84**:417–424.

Adjobo-Hermans MJW, Goedhart J, van Weeren L, Nijmeijer S, Manders EMM, Offermanns S, and Gadella Jr TWJ (2011) Real-time visualization of heterotrimeric G protein Gq activation in living cells. *BMC Biol* **9**:32.

Aronson JK (2016) Cyclobenzaprine, in *Meyler's Side Effects of Drugs,* 16th ed (Aronson JK ed) p. 781, Elsevier.

Bakker RA, Schoonus SBJ, Smit MJ, Timmerman H, and Leurs R (2001) Histamine H(1)-receptor activation of nuclear factor-κ B: roles for G β γ- and G α(q/11)-subunits in constitutive and agonist-mediated signaling. *Mol Pharmacol* **60**:1133–1142.

Barnes CD (1976) Effects of cyclobenzaprine on brainstem motor systems. *Neuropharmacology* **15**:643–652.

Barnes CD and Adams WL (1978) Effects of cyclobenzaprine on interneurones of the spinal cord. *Neuropharmacology* **17**:445–450.

Barnes CD, Fung SJ, and Gintautas J (1980) Brainstem noradrenergic system depression by cyclobenzaprine. *Neuropharmacology* **19**:221–224.

Bebarta VS, Maddry J, Borys DJ, and Morgan DL (2011) Incidence of tricyclic antidepressant-like complications after cyclobenzaprine overdose. *Am J Emerg Med* **29**:645–649.

Booth, R. G. and N. H. Moniri (2005) Ligand-directed multifunctional signaling of histamine H1 receptors. *Inflamm Res* **54** (Suppl 1):S44–S45.

Booth RG, Moniri NH, Bakker RA, Choksi NY, Nix WB, Timmerman H, and Leurs R (2002) A novel phenylaminotetralin radioligand reveals a subpopulation of histamine H(1) receptors. *J Pharmacol Exp Ther* **302**:328–336.

Burns RN and Moniri NH (2011) Agonist- and hydrogen peroxide-mediated oxidation of the β2 adrenergic receptor: evidence of receptor s-sulfenation as detected by a modified biotin-switch assay. *J Pharmacol Exp Ther* **339**:914–921.

Burns RN, Singh M, Senatorov IS, and Moniri NH (2014) Mechanisms of homologous and heterologous phosphorylation of FFA receptor 4 (GPR120): GRK6 and PKC mediate phosphorylation of Thr^{347}, Ser^{350}, and Ser^{357} in the C-terminal tail. *Biochem Pharmacol* **87**:650–659.

Chang RSL, Tran VT, and Snyder SH (1978) Histamine H1-receptors in brain labeled with 3H-mepyramine. *Eur J Pharmacol* **48**:463–464.

Chang RSL, Tran VT, and Snyder SH (1979) Characteristics of histamine H1-receptors in peripheral tissues labeled with [3H]mepyramine. *J Pharmacol Exp Ther* **209**:437–442.

Cheng Y and Prusoff WH (1973) Relationship between the inhibition constant (K1) and the concentration of inhibitor which causes 50 per cent inhibition (I50) of an enzymatic reaction. *Biochem Pharmacol* **22**:3099–3108.

de Leon J and Nikoloff DM (2008) Paradoxical excitation on diphenhydramine may be associated with being a CYP2D6 ultrarapid metabolizer: three case reports. *CNS Spectr* **13**:133–135.

Gintautas J and Barnes CD (1979) Effects of cyclobenzaprine on the locus ceruleus. *Proc West Pharmacol Soc* **22**:37–41.

Hall DA and Langmead CJ (2010). Matching models to data: a receptor pharmacologist's guide. *Br J Pharmacol* **161**:1276–1290.

Honda M, Nishida T, and Ono H (2003) Tricyclic analogs cyclobenzaprine, amitriptyline and cyproheptadine inhibit the spinal reflex transmission through 5-HT(2) receptors. *Eur J Pharmacol* **458**:91–99.

Kachur JF, Allbee WE, and Gaginella TS (1988) Antihistaminic and antimuscarinic effects of amitriptyline on guinea pig ileal electrolyte transport and muscle contractility in vitro. *J Pharmacol Exp Ther* **245**:455–459.

Kanba S and Richelson E (1984) Histamine H1 receptors in human brain labelled with [3H]doxepin. *Brain Res* **304**:1–7.

Kurko D, Bekes Z, Gere A, Baki A, Boros A, Kolok S, Bugovics G, Nagy J, Szombathelyi Z, and Ignácz-Szendrei G (2009) Comparative pharmacology of adrenergic α(2C) receptors coupled to Ca(2+) signaling through different Galpha proteins. *Neurochem Int* **55**:467–475.

Lang IM and Barnes CD (1982) The effects of cyclobenzaprine on locus coeruleus cells in vitro. *Proc West Pharmacol Soc* **25**:361–363.

Lang IM and Barnes CD (1983) Cyclobenzaprine effects on locus coeruleus cells in tissue slice. *Neuropharmacology* **22**:249–252.

Langer I, Perret J, Vertongen P, Waelbroeck M, and Robberecht P (2001) Vasoactive intestinal peptide (VIP) stimulates [Ca2+]i and cyclic AMPin CHO cells expressing Galpha16. *Cell Calcium* **30**:229–234.

Matsumoto Y, Funahashi J, Mori K, Hayashi K, and Yano H (2008) The noncompetitive antagonism of histamine H1 receptors expressed in Chinese hamster ovary cells by olopatadine hydrochloride: its potency and molecular mechanism. *Pharmacology* **81**:266–274.

McCarberg B, Altman C, and Ma Y (2011) Independence of efficacy and drowsiness with cyclobenzaprine extended-release for the treatment of acute low back and neck spasm. *J Pain* **12** (Suppl):P46.

Moguilevsky N, Varsalona F, Guillaume JP, Noyer M, Gillard M, Daliers J, Hénichart JP, and Bollen A (1995) Pharmacological and functional characterisation of the wild-type and site-directed mutants of the human H1 histamine receptor stably expressed in CHO cells. *J Recept Signal Transduct Res* **15**:91–102.

Moguilevsky N, Varsalona F, Noyer M, Gillard M, Guillaume JPP, Garcia L, Szpirer C, Szpirer J, and Bollen A (1994) Stable expression of human H1-histamine-receptor cDNA in Chinese hamster ovary cells. Pharmacological characterisation of the protein, tissue distribution of messenger RNA and chromosomal localisation of the gene. *Eur J Biochem* **224**:489–495.

Moniri, N. H. and R. G. Booth (2004) Functional heterogeneity of histamine H1 receptors. *Inflamm Res* **53** (Suppl 1):S71–S72.

Moniri NH, Covington-Strachan D, and Booth RG (2004) Ligand-directed functional heterogeneity of histamine H1 receptors: novel dual-function ligands selectively activate and block H1-mediated phospholipase C and adenylyl cyclase signaling. *J Pharmacol Exp Ther* **311**:274–281.

Moniri NH and Daaka Y (2007) Agonist-stimulated reactive oxygen species formation regulates β2-adrenergic receptor signal transduction. *Biochem Pharmacol* **74**:64–73.

Muramatsu H, Sawanishi H, Iwasaki N, Kakiuchi M, Ohashi T, Kato H, and Ito Y (1993) Study on zwitter-ionization of drugs. II. Synthesis and pharmacological activity of some N-[3-(5H-dibenzo[a, d]cyclohepten-5-ylidene) propyl]-N-methylamino- and N-[3-(6H-dibenz[b, e]oxepin-11-ylidene) propyl]-N-methylamino-alkanoic acid derivatives and related compounds. *Chem Pharm Bull (Tokyo)* **41**:1987–1993.

Olsen RHJ, DiBerto JF, English JG, Glaudin AM, Krumm BE, Slocum ST, Che T, Gavin AC, McCorvy JD, Roth BL et al. (2020) TRUPATH, an open-source biosensor platform for interrogating the GPCR transducerome. *Nat Chem Biol* **16**:841–849.

Richelson E and Nelson A (1984) Antagonism by antidepressants of neurotransmitter receptors of normal human brain in vitro. *J Pharmacol Exp Ther* **230**:94–102.

Senatorov IS, Cheshmehkani A, Burns RN, Singh K, and Moniri NH (2020) Carboxy-terminal phosphoregulation of the long splice isoform of free-fatty acid receptor-4 mediates β-arrestin recruitment and signaling to ERK1/2. *Mol Pharmacol* **97**:304–313.

Share NN and McFarlane CS (1975) Cyclobenzaprine: novel centrally acting skeletal muscle relaxant. *Neuropharmacology* **14**:675–684.

Shihata AMA (2021) Determination of cyclobenzaprine and N-desmethylcyclobenzaprine, chlorpheniramine and its analog in liver tissues. *MAR Pharmacology and Toxicology* **2**:1–10.

Shimamura T, Shiroishi M, Weyand S, Tsujimoto H, Winter G, Katritch V, Abagyan R, Cherezov V, Liu W, Han GW et al. (2011) Structure of the human histamine H1 receptor complex with doxepin. *Nature* **475**:65–70.

Singh M and Moniri NH (2012) Reactive oxygen species are required for β2 adrenergic receptor-β-arrestin interactions and signaling to ERK1/2. *Biochem Pharmacol* **84**:661–669.

Spiller HA and Cutino L (2003) Fatal cyclobenzaprine overdose with postmortem values. *J Forensic Sci* **48**:883–884.

Stables J, Green A, Marshall F, Fraser N, Knight E, Sautel M, Milligan G, Lee M, and Rees S (1997) A bioluminescent assay for agonist activity at potentially any G-protein-coupled receptor. *Anal Biochem* **252**:115–126.

Teva Pharmaceuticals USA, Inc. (2013) AMRIX(R) oral extended-release capsules, cyclobenzaprine HCl oral extended release capsules [package insert and prescribing information].

Tran VT, Chang RSL, and Snyder SH (1978) Histamine H1 receptors identified in mammalian brain membranes with [3H]mepyramine. *Proc Natl Acad Sci USA* **75**: 6290–6294.

Winek Jr CL, Wahba WW, and Winek CL (1999) Drowning due to cyclobenzaprine and ethanol. *Forensic Sci Int* **100**:105–108.

Zhu T, Fang L-Y, and Xie X (2008) Development of a universal high-throughput calcium assay for G-protein- coupled receptors with promiscuous G-protein Galpha15/16. *Acta Pharmacol Sin* **29**:507–516.

Address correspondence to: Dr. Nader H. Moniri, Department of Pharmaceutical Sciences, College of Pharmacy, Mercer University Health Sciences Center, Mercer University, 3001 Mercer University Drive, Atlanta, GA 30341. E-mail: moniri_nh@mercer.edu